Tl^{2+} EPR study of the dynamics of the proton-glass transition in $Rb_{1-x}(NH_4)_xH_2PO_4$

R. Kind, R. Blinc,* J. Dolinsek,* and N. Korner
Eidgenössische Technische Hochschule Zürich-Hönggerberg, Institut für Quantenelektronik, CH-8093 Zürich, Switzerland

B. Zalar
Jožef Stefan Institute, University of Ljubljana, YU-61111 Ljubljana, Yugoslavia

P. Cevc,* N. S. Dalal, and J. DeLooze
Chemistry Department, University of West Virginia, Morgantown, West Virginia 26505
(Received 9 April 1990)

The temperature dependence of the Tl^{2+} EPR line shapes and second moments in Tl-doped $Rb_{1-x}(NH_4)_xH_2PO_4$ between 160 and 10 K allows for a direct determination of the static and dynamic features of the glass transition in this system. The static features can be described by a random-field smearing of a random-bond Ising pseudo-spin-glass transition with a nominal glass temperature of $T_G=30$ K and a random-field contribution of $T_f=60$ K, whereas the dynamic features show up on a slowing down of the proton intra O—H $\cdots$ O bond motion. The comparison of the theoretical and experimental line shapes provides a check of the validity of a recently developed dynamic approach to the local-polarization distribution and magnetic-resonance line shape in proton and deuteron glasses.

I. INTRODUCTION

It is well established by now[1-3] that, in contrast to magnetic spin glasses, the freezing transition into the so-called proton-glass phase[4] in mixed ferroelectric and antiferroelectric hydrogen-bonded crystals as RADP-x and DRADP-x [$Rb_{1-x}(NH_4)_xH_2PO_4$ and $Rb_{1-x}(ND_4)_xD_2PO_4$, respectively] occurs in the presence of quenched random local fields.[1-6] It has also been shown that the second moment of the inhomogeneous NMR (Ref. 1) or EPR (Ref. 7) line-shape frequency distribution function allows—in the fast-motion limit[1,2]—a direct experimental determination of the Edwards-Anderson order parameter of the proton or deuteron pseudo-spin-glass phase.

Whereas the static aspects of the proton-glass transition are thus slowly becoming better understood, relatively little progress has been made in understanding the dynamics[8,9] of this transition. Early NMR spin-lattice-relaxation-time measurements[10-12] have shown a tremendous slowing down of the O—H $\cdots$ O and O—D $\cdots$ O proton and deuteron dynamics on cooling into the glass phase. Such a slowing down has not been observed before in pure hydrogen-bonded ferroelectric or antiferroelectric crystals and represents one of the characteristic features of the glass transition.

The slowing down of the order-parameter dynamics on cooling into the glass phase affects the NMR line shape[1,2] as well and makes a discrimination between a static glass transition or a kinetic slowing down rather difficult. The dynamic corrections to the NMR line shape[1,2] become important at the crossover from the fast- to the slow-motion limit. This occurs in a temperature range where the frequency of reorientation of the elementary O—H $\cdots$ O pseudospins (i.e., the frequency of intrabond proton jumping) becomes comparable to the frequency splitting $2\omega_1$ of the NMR line for the proton being frozen out in the left- or right-hand side of the O—H $\cdots$ O double-minimum potential, respectively.

In Rb or deuteron NMR (Refs. 1 and 2) of proton glasses, the frequency splitting $2\omega_1$ is in the 10^4-10^5 Hz range and the crossover from the fast- to the slow-motion limit[1,2,11] occurs at relatively low temperatures. These probes are thus mainly sensitive to the static aspects of the glass transition as most of the investigated temperature range corresponds to the fast-motion limit. To check on the dynamic aspects of the proton-glass transition, it is therefore convenient to use probes where $2\omega_1$ is large enough to shift the crossover between the fast- and the slow-motion regime to higher temperatures.

Such a probe is provided by the Tl^{2+} paramagnetic center which replaces the Rb ions while keeping the symmetry of the cation site[13]—in view of dynamic charge compensation—at high enough temperatures. At lower temperatures, the dynamic charge compensation becomes slow on the EPR time scale thus leading to an additional splitting of the Tl^{2+} EPR lines if the magnetic field does not lie in the a-b plane. In the a-b plane no additional line splitting is seen and the Tl^{2+} ion effectively keeps the symmetry of the cation site down to $T\rightarrow 0$. For $\mathbf{B}_0\|\langle 100\rangle$ and $\mathbf{B}_0\|\langle 110\rangle$, the Tl^{2+} EPR spectrum[7,13-16] exhibits, at 160 K, two lines, a low-field one and a high-field one which both split into doublets at lower temperatures. The two doublet splittings are of different magnitudes. The low-field one amounts to $\omega_{1L}=(2\pi)440$ MHz and the high-field one to $\omega_{1H}=(2\pi)669$ MHz.

In addition to a higher ω_1 and thus a higher crossover temperature from the fast- to the slow-motion regime, the Tl^{2+} probe provides us with two different natural clocks ω_{1L} and ω_{1H} for the measurement of the pseudospin dy-

namics. If the glass transition is entirely static, the splitting of the two doublets should occur at the same temperature and the ratio of the second moments of high- and low-field lines should amount to

$$\frac{M_{2H}}{M_{2L}}=\left[\frac{\omega_{1H}}{\omega_{1L}}\right]^2 . \tag{1}$$

For a purely dynamic freezeout, on the other hand, the high-field singlet-doublet transition with $\omega_{1H}=(2\pi)669$ MHz should take place at a higher temperature than the low-field one where $\omega_{1L}=(2\pi)440$ MHz. In addition, the ratio of the observable second moments of the high- and the low-field transition should not be constant but should vary with temperature from $(\omega_{1H}/\omega_{1L})^3$ in the fast-motion limit to $(\omega_{1H}/\omega_{1L})^2$ in the slow-motion limit, as we will show later on.

Here we present a comparison of experimental and theoretical line shapes and second moments for (a) the purely static case, (b) the purely dynamic case, and (c) the case where both static and dynamic aspects of the glass transition influence the EPR line shape. We hope that the results might throw some new light on the dynamic aspects of the transition in proton glasses and thus help to close the conceptual gap between spin glasses and ordinary glasses.

II. EXPERIMENT

Single crystals of $Rb_{1-x}(NH_4)_xH_2PO_4$ with $x=0.34$, 0.43, and 0.70 doped with Tl^+ (approx 1% molar concentration) were grown from a water solution. The Tl^{2+} centers were created by γ irradiation of the doped samples at liquid-nitrogen temperature. The centers proved to be stable up to 160 K. Above this temperature they begin to disappear as seen from the intensity of the EPR lines.

In a virgin RbH_2PO_4 crystal (tetragonal modification) the Tl^+ ions replace the Rb ions without affecting the cation site symmetry. The Tl^{2+} center, however, can keep the cation site symmetry only by dynamic charge compensation. It has been shown for the case of Tl^{2+}-doped KH_2PO_4 that the cation site symmetry is maintained down to low temperatures and that deviations from this symmetry were observed only at 4 K.[13,15] As mentioned above, we have chosen for our measurements a direction of the external magnetic field $\mathbf{B}_0$ in the *a*-*b* plane of the crystal so that the slowing down of the dynamic charge transfer does not affect the EPR line shape.

The Tl^{2+} (ground state $^2S_{1/2}$) EPR spectra are described by the spin Hamiltonian[13–16]

$$\mathcal{H}=\mathbf{S}\cdot\mathsf{A}_{op}\cdot\mathbf{I}+\mathbf{B}_0\cdot\mathsf{g}_{op}\cdot\mathbf{S} , \tag{2}$$

where $S=\frac{1}{2}$, $I=\frac{1}{2}$, and the hyperfine interaction A_{op} is so large that the Zeeman term $\mathbf{B}_0\cdot\mathsf{g}_{op}\cdot\mathbf{S}$ is only a small perturbation. The energy levels are characterized by the quantum numbers $F=I\pm S=0,1$ and the magnetic quantum numbers $m_F=0,\pm1$.

We shall now discuss the relation between the EPR line splitting and the spontaneous polarization p for the paraelectric-ferroelectric transition in Tl^{2+}-doped RbH_2PO_4. There are two chemically equivalent Rb sites per primitive unit cell ($Z=2$) which transform into each other by the glide planes $\{110\}$ of both the high-temperature tetragonal space group $I\bar{4}2d$ and the low-temperature orthorhombic space group $Fdd2$. In the high-temperature paraelectric phase the O—H $\cdots$ O protons are dynamically disordered between the two equilibrium sites in the hydrogen bonds. Since both Rb sites have the symmetry $\bar{4}$, they cannot be distinguished by an EPR measurement involving a second rank tensor such as the hyperfine interaction. In the ferroelectric phase this symmetry is reduced to a twofold axis 2_z, whereas it is lost completely in the antiferroelectric phase of $NH_4H_2PO_4$ which has the space group $P2_12_12_1$ with $Z=4$. As a result of the proton ordering, the two Rb sites become physically—but not chemically—inequivalent and the Tl^{2+} transitions split at T_c into doublets as indeed observed for the orientations $\mathbf{B}_0\|\langle100\rangle$ and $\mathbf{B}_0\|\langle110\rangle$.[13–15] For other orientations, $\mathbf{B}_0\perp\langle001\rangle$ four lines are observed. This is due to the existence of 90° domains related by the lost fourfold symmetry axis of the paraelectric phase. The most important symmetry elements which are lost during the phase transition are the twofold axes 2_x and 2_y which are located at the center of the hydrogen bonds. These operations are not only responsible for the average symmetry of the O—H $\cdots$ O bonds but they also relate the two Rb sites which become physically inequivalent at the phase transition and give rise to the Tl^{2+} EPR line splitting below T_c. If this lost symmetry operation is applied to a ferroelectric domain, not only the spontaneous polarization is reversed, but also the two lines in the doublets are exchanged. Their positions are thus directly connected with the spontaneous polarization $\pm p$—which is the order parameter of the ferroelectric transition—and can thus correspondingly be assigned as ω^+ and ω^-. It is useful to expand the EPR line shift in powers of the polarization p and to separate symmetric and antisymmetric terms by the well-known relations

$$(\omega^+ +\omega^-)/2=\omega_0+\omega_2 p^2+\omega_4 p^4+\cdots$$

and (3)

$$(\omega^+ -\omega^-)/2=\omega_1 p+\omega_3 p^3+\cdots .$$

From the temperature dependence of the spectrum one can conclude that the symmetric terms in p are negligible, i.e., $\omega_4\ll\omega_2\approx0$. We can safely assume that the linear term ($\omega_1 p$) is dominant. The constants ω_{1L} and ω_{1H} can thus be determined from the EPR line splitting at low temperatures.

Similarly one can treat the antiferroelectric case of $NH_4H_2PO_4$ (ADP). Here too we have for the orientations $\mathbf{B}_0\|\langle100\rangle$ and $\mathbf{B}_0\|\langle110\rangle$ only two lines corresponding to antiferroelectric antiphase domains, i.e., we have

$$(\omega^+ -\omega^-)/2=\omega_1^{AFE}p_{AFE}+\omega_3^{AFE}p_{AFE}^3+\cdots , \tag{4}$$

where p_{AFE} is the antiferroelectric order parameter, i.e., the spontaneous sublattice polarization. Here, too, the third-order term can be neglected.

Experiments have established that the two correspond-

ing ω_1's in RDP and ADP, respectively, are equal within the resolution of the method, i.e., we have $\omega_1^{\mathrm{AFE}} \approx \omega_1^{\mathrm{FE}}$.[17] This is a very important result which demonstrates that the Tl^{2+} doublet splittings are nearly identical in ferroelectric RDP and in antiferroelectric ADP. This means that the Tl^{2+} center is, in fact, a local probe which reflects the O—H · · · O proton ordering, similar to the O—D · · · O deuteron resonance in DRADP, and is not selectively sensitive to ferroelectric or antiferroelectric clusters.

Here we have measured the temperature dependence of the Tl^{2+} EPR line shape in $Rb_{1-x}(NH_4)_xH_2PO_4$ for $\mathbf{B}_0 \| \langle 110 \rangle$ at various temperatures between 4 and 160 K for the compositions $x = 0.34$ and 0.70, i.e., for compositions where no long-range ferroelectric or antiferroelectric order takes place at low temperatures. The two-clock experiment described in Sec. I has been performed on a crystal with the composition $x = 0.43$ for $\mathbf{B}_0 \| \langle 110 \rangle$ at various temperatures between 87 and 160 K. Similarly, we have checked whether the ^{87}Rb NMR line shape transition in RADP-43 depends on the doping with Tl^{2+} or not. Here we found that the line-shape transition temperature does not differ between doped and undoped RADP for Tl^{2+} concentrations similar to the ones used in the EPR experiment.

III. THEORY

The O—H · · · O bond represents here a two-position reorientable dipole which can be described by an Ising pseudospin $S^z = \pm 1$. The simplest model capable of describing the transition in proton glasses is the Ising pseudospin model with infinitely ranged random-bond interactions and quenched random fields:[3]

$$\mathcal{H} = -\tfrac{1}{2} \sum_{ij} J_{ij} S_i^z S_j^z - \sum_i f_i S_i^z \ , \tag{5}$$

where the random interactions J_{ij} and random fields f_i are assumed to be independently distributed according to their respective Gaussian probability densities:

$$P(J_{ij}) = \frac{1}{J\sqrt{2\pi}} \exp(-\tfrac{1}{2} J_{ij}^2 / J^2)$$

and (6)

$$P(f_i) = \frac{1}{\sqrt{2\pi\Delta}} \exp(-\tfrac{1}{2} f_i^2 / \Delta) \ .$$

The dominant contribution to the EPR frequency shift for a given Tl^{2+} site i arises from the eight nearest O—H · · · O bonds. If the motion of the acid O—H · · · O protons between the two equilibrium sites is fast on the EPR time scale, i.e., fast compared to the doublet splitting $2\omega_1$, the Tl^{2+} ions "see" only the time-averaged proton positions. In this fast-motion limit we have

$$\omega_i = \omega_{0,i} + \sum_{j=1}^{8} c_j p_j, \quad 2\omega_1 \tau_0 \ll 1 \ , \tag{7a}$$

where $p_j = \langle S_j^z \rangle$ is the local polarization, i.e, the time-averaged value of S_j^z, $\omega_1 \approx 2\pi \sum_j c_j$, and τ_0 is the characteristic O—H · · · O intrabond reorientation time. Since the motion of the eight protons around the Tl^{2+} center is highly correlated so that $p_i = p_j = p$, one can characterize the whole cluster by a single p value in the interval -1 to $+1$. In this case expression (7a) simplifies to

$$\omega_i = \omega_{0,i} + \omega_1 p \ . \tag{7b}$$

In the paraelectric phase far above the glass transition, we have $p = 0$ and $\omega_i = \omega_{0,i}$. In the slow-motion limit, on the other hand, the Tl^{2+} ions "see" the instantaneous proton position in the O—H · · · O bonds so that, maintaining the correlations, we get

$$\omega_i = \omega_{0,i} \pm \omega_1, \quad p = \pm 1, \quad 2\omega_1 \tau_0 \gg 1 \ . \tag{7c}$$

If the singlet-doublet transition is a purely static effect, reflecting the equilibrium glass transition, the situation is as follows: As long as the O—H · · · O proton intrabond reorientation frequency τ_0^{-1} is high as compared to the rigid lattice double splitting frequency $2\omega_1$, we are in the fast-motion regime and expression (7b) applies. The EPR probes see different local polarizations at different parts of the crystal resulting in an inhomogeneous line broadening which reflects the probability distribution of the local polarizations $W(p)$. We get

$$I(\omega) d\omega = W(p) dp \ , \tag{8}$$

where $I(\omega)$ is the average frequency distribution function characterizing the inhomogeneous EPR line shape and $W(p)$ is the local polarization distribution function. For the Hamiltonian (5), $W(p)$ is given by[1,2]

$$W(p) = \frac{1}{\beta J [2\pi(q + \tilde{\Delta})]^{1/2}} \frac{1}{1 - p^2} \times \exp\left[-\frac{1}{2} \frac{\operatorname{arctanh}^2(p)}{\beta^2 J^2 (q + \tilde{\Delta})} \right] , \tag{9}$$

where $\beta = 1/k_B T$, $\tilde{\Delta} = \Delta / J^2$, and the Edwards-Anderson order parameter $q = q_{\mathrm{EA}}$ is given by the self-consistency equation[3]

$$q = \frac{1}{\sqrt{2\pi}} \int dz \exp(-z^2/2) \tanh^2[\beta J (q + \tilde{\Delta})^{1/2} z] \ . \tag{10}$$

For a linear relation between ω and p such as (7b), the frequency distribution $I(\omega)$ directly reflects the local-polarization distribution $W(p) = \omega_1^2 I(\omega)$. For very high temperatures $T \gg T_G = J/k_B$, $W(p)$ becomes a δ function centered at $p = 0$. At $T = T_G$, $W(p)$ flattens out and for $T < T_G$, $W(p)$ exhibits a two-peaked structure[1,2] with maxima at $p = \pm 1$.

The above considerations are valid in the fast-motion regime. At the transition to the slow-motion regime we have to take into account the additional broadening due to the slowing down of the fluctuations. The resulting line shape is now[1,2]

$$I(\omega) = \int_{-1}^{+1} I(\omega, p) W(p) dp \ , \tag{11}$$

where $I(\omega, p)$ is[2]

$$I(\omega, p) = \frac{1}{\pi} \frac{\Gamma \omega_1^2 (1 - p^2)}{(\omega^2 - \omega_1^2)^2 + \Gamma^2 (\omega - \omega_1 p)^2} \ . \tag{12}$$

The function $I(\omega,p)$ represents the line shape[1,2] due to proton (or deuteron) chemical exchange in an asymmetric two-site potential. It can be measured by two-dimensional NMR. Here Γ is the pseudo-spin-flip rate. For thermally activated intrabond jumps across a potential barrier E_a in an asymmetric two-site potential, one finds[2]

$$\Gamma=\frac{1}{\tau_c}=\frac{\Gamma_0}{(1-p^2)^{1/2}} ,$$

where

$$\frac{1}{\Gamma_0}=\tau_0=\tau_\infty\exp(\beta E_a) \tag{13}$$

with τ_∞ playing the role of an inverse attempt frequency. The case $\Gamma_0>2\omega_1$ corresponds to the fast-motion regime where the characteristic EPR time $\tau_{\rm EPR}=1/2\omega_1$ is longer than the correlation time $\tau_0=\tau_c$ $(p=0)$, whereas the slow-motion regime corresponds to $\Gamma_0<2\omega_1$. Since Γ diverges for $p\pm1$, some of the bonds will always be in the fast-motion regime even if $\Gamma_0<2\omega_1$. $I(\omega)$ reduces to $W(p)/\omega_1$ in the fast-motion limit where $I(\omega,p)$ becomes a δ function:

$$I(\omega,p)=\delta(\omega-\omega_1 p) . \tag{14}$$

The line shape $I(\omega)$ will thus change from a Gaussian at high temperatures to a double-peaked structure at low temperatures.

The observable or truncated second moment $M_2^{\rm tr}$, i.e., the second moment evaluated over a finite frequency range, e.g., $-3\omega_1<\omega<+3\omega_1$, is in the fast-motion limit proportional to the Edwards-Anderson order parameter $q_{\rm EA}$ (Ref. 2)

$$M_2^{\rm tr}=\int_{-a}^{+a} I(\omega)\omega^2 d\omega=\omega_1^2 q_{\rm EA},\quad a>\omega_1 , \tag{15}$$

whereas it is in the slow-motion limit given by

$$M_2^{\rm tr}=M_2=\omega_1^2 \tag{16}$$

independently of $q_{\rm EA}$. In the intermediate range between the fast- and the slow-motion limits, $M_2^{\rm tr}$ will deviate from $(q_{\rm EA}\omega_1^2)$. The deviation will depend on ω_1 as well as on Γ. The temperature dependence of $M_2^{\rm tr}$ is, in this range, best obtained by numerically evaluating Eq. (15) in a finite-frequency interval, e.g., for $-3\omega_1<\omega<+3\omega_1$.

If, on the other hand, the glass transition is of purely kinetic origin and the singlet-doublet transition is only a motional averaging effect reflecting the slowing down of the proton motion in the O—H $\cdots$ O bonds, the EPR line shape should be homogeneous rather than inhomogeneous and given by $I(\omega,p)$ for $p=0$, i.e., by the corresponding modification of the function (12). In the slow-motion limit $2\omega_1\tau_0\gg1$, we now have two pseudo-Lorentzians centered at $\pm\omega_1$, whereas a single pseudo-Lorentzian line centered at zero is found in the fast-motion limit $2\omega_1\tau_0\ll1$. The transition between these two regimes occurs when $2\omega_1\tau_0\approx1$. We call these line shapes pseudo-Lorentzians because the total second moment of $I(\omega,p=0)$ is always finite and amounts to ω_1^2 independently of the value of Γ, whereas the second moment of a true Lorentzian is known to be infinite.

The truncated or observable second moment of the line $M_2^{\rm tr}$, however, depends strongly on the rate Γ as long as we are far from the slow-motion limit where $M_2^{\rm tr}$ converges to ω_1^2 from below. In the fast-motion limit the expression

$$M_2^{\rm tr}=\int_{-3\omega_1}^{+3\omega_1} I(\omega,p=0)\omega^2 d\omega \tag{17}$$

can be evaluated analytically and one obtains

$$M_2^{\rm tr}=\frac{2\Gamma\omega_1^2}{\pi(\Gamma^2-2\omega^2)^{1/2}}\arctan\left[\frac{3\omega_1}{(\Gamma^2-2\omega^2)^{1/2}}\right]\approx\frac{6\omega_1^3}{\pi\Gamma} . \tag{18}$$

We have thus proved that the ratio M_{2H}/M_{2L} indeed equals $(\omega_{1H}/\omega_{1L})^3$ in the fast-motion limit for the two-clock experiment as claimed in Sec. I. For the transition range $2\omega_1\tau_0\approx1$, $M_2^{\rm tr}$ can be obtained from numerical integration.

IV. RESULTS AND DISCUSSION

Both the low- and the high-field Tl^{2+} EPR lines in RADP for $\mathbf{B}_0\|\langle 110\rangle$ change from high-temperature singlets to low-temperature doublets. The temperature dependence of the two (i.e., low- and high-field ones) Tl^{2+} EPR doublet splittings for $x=0.43$ is presented in Fig. 1. In this presentation, the two doublets are shown superposed whereas, in reality, they are well separated by approximately 850 G. The position of the lines was determined by fitting two Gaussians to the measured line shapes $I(B_0)$. For small splittings this fit procedure becomes unstable and the error in the calculated line positions exceeds the splitting. Nevertheless, one can see unambiguously that the two doublets converge to a single line at the same temperature of about 130 K, i.e., in this presentation of the data no dynamic effects can be observed. On the other hand, a ^{87}Rb NMR singlet-doublet transition was observed around 60 K in an undoped

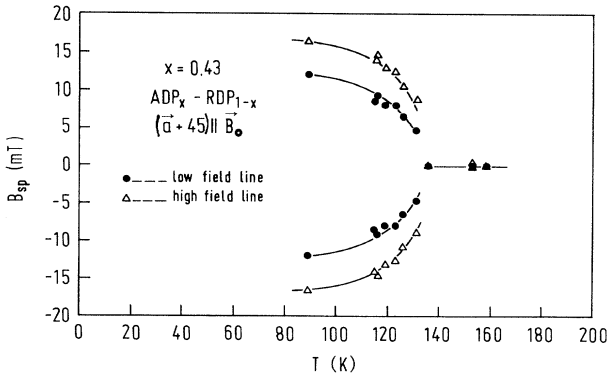

FIG. 1. Temperature dependence of the splitting of the low- and high-field EPR doublets in Tl^{2+}-doped RADP.

RADP crystal with $x=0.35$ already some years ago.[18]

There are two possible explanations for the big difference in the EPR and NMR line-shape transition temperatures, a kinetic one and a static one. The arguments for a line-shape transition induced by a kinetic slowing down have already been discussed in Sec. III. As mentioned before, the relevant ω_1 amounts to approximately 10^5 s^{-1} for the ^{87}Rb central transition in RADP. The big ratio of about 3×10^4 between the EPR and the NMR line splittings could well account for such a difference in the transition temperatures. On the other hand, the Tl^{2+} centers could affect the static behavior of the crystal by a strong enhancement of the local random fields. An enhancement of the random-field variance Δ by a factor of four would be sufficient to account for the effect. In order to check on the influence of the Tl^{2+} centers, we have performed ^{87}Rb NMR measurements on doped and undoped RADP crystals described in Sec. II. The results are unambiguous: changes in the static behavior due to the Tl^{2+} doping can safely be ruled out. Whereas, we know from the two-clock experiment, that the EPR line-shape transition must have a static component due to glassy proton ordering, the comparison with the ^{87}Rb NMR clearly indicates the presence of dynamic effects too. We thus have to deal with a superposition of both static glassy-type ordering and kinetic slowing down.

The temperature dependence of the reduced second moment of the low-field EPR doublet line shape

$$I(B_{sp}/B_{max})=I(\omega/\omega_1)$$

of RADP ($x=0.70$) is shown in Fig. 2. The most important feature in this temperature dependence is the rounding off to a plateau below 50 K. The existence of this plateau clearly indicates that we have reached the slow-motion limit where the reduced second moment has the value 1.0 which corresponds to the value B^2_{max} or ω_1^2 for the unreduced second moments. The plateau thus serves as a calibration of the magnitude of M_2^{tr} which is needed for the composition with the Edwards-Anderson order parameter q_{EA}. The solid line is the theoretical temperature dependence of M_2^{tr} obtained by a numerical evaluation of the truncated second moment of expression (11). There are four fit parameters in this calculation, two for the statics and two for the dynamics. For the statics we had to determine the two variances J^2 and Δ of the random interactions and of the random fields, respectively, which can also be expressed in terms of temperature ($J=k_BT_G$ which is the nominal spin-glass temperature for $\Delta=0$, and $\sqrt{\Delta}=k_BT_f$). Here we found $T_G=30$ K and $T_f=60$ K. For the dynamic parameter we found an activation energy of $E_a=24$ meV and the inverse attempt frequency of $\tau_\infty=7.6\times10^{-12}$ s.

For comparison we show also the temperature dependences of the calculated second moments M_2^{tr} for the pure static case, i.e., q_{EA} (dashed line) and the pure kinetic case (dash-dotted line) using the above static or dynamic parameters, respectively.

In Fig. 3, the measured EPR line shape for a crystal with $x=0.70$ for $T=150$ K is compared with the calculated line shape using the above four parameters, i.e., including static and dynamic effects of the phase transition. Both line shapes are normalized, i.e., their zeroth moments equal one ($M_0=1.0$). The agreement between

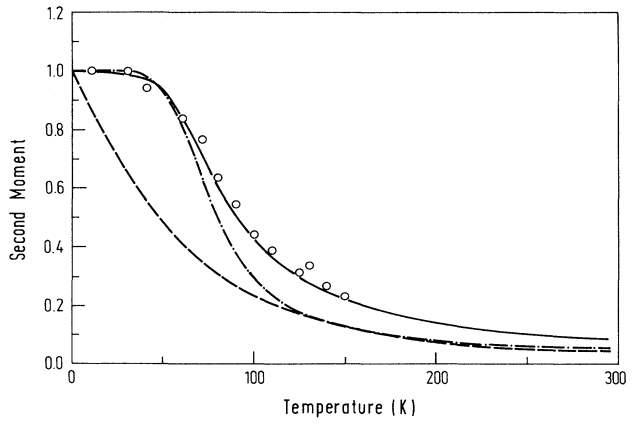

FIG. 2. Temperature dependence of the reduced second moment of the low-field Tl^{2+} EPR doublet in RADP. The experimental results (circles) are compared with theoretical fits for the pure static case (dashed line) according to Eqs. (8) and (9), the pure dynamic case (dash-dotted line) according to Eq. (12) with $p=0$, and the case given by expression (11) (solid line) where both static and dynamic effects are taken into account. The static fit parameters are $T_G=30$ K and $T_f=60$ K, while the dynamic fit parameters are $E_a=24$ meV and $\tau_\infty=7.6\times10^{-12}$ s.

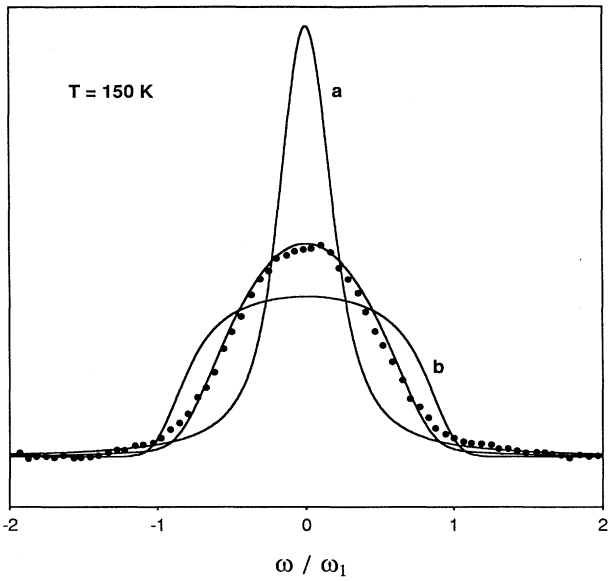

FIG. 3. Comparison of the experimental Tl^{2+} EPR line shape in RADP with $x=0.7$ at $T=150$ K (solid circles) with the theoretical curves for (a) the pure dynamic case and (b) the pure static case and the matching case where both static and dynamic effects are taken into account. The calculations were performed using the fit parameters obtained from the second moment data.

theory and experiment is nearly perfect. We would like to emphasize that this agreement is not the result of a line-shape fit. Only the four fit parameters obtained from the second moment fit were used in the calculation. For comparison we also show that no agreement between experimental and theoretical line shapes can be obtained for the pure dynamic (a) and the pure static (b) cases. Here we compared normalized line shapes with equal truncated second moments of the above values of the static or dynamic parameters, respectively. However, to obtain the same second moments they had to be calculated for lower temperatures, i.e., around 100 K as seen from Fig. 2. This comparison once more confirms the coexistence of both kinetic slowing down and static glassy-type ordering in RADP.

In Fig. 4 we compare measured and calculated line shapes for several temperatures from 10 to 150 K. In order to obtain a better agreement between measured and calculated line shapes at low temperatures, we had to introduce an additional parameter σ_0 that takes care of the nonlocal static effects connected with the glass ordering. It was shown[1] that the second moment of the inhomogeneously broadened NMR line shapes in a proton glass is proportional to the Edwards-Anderson order parame-

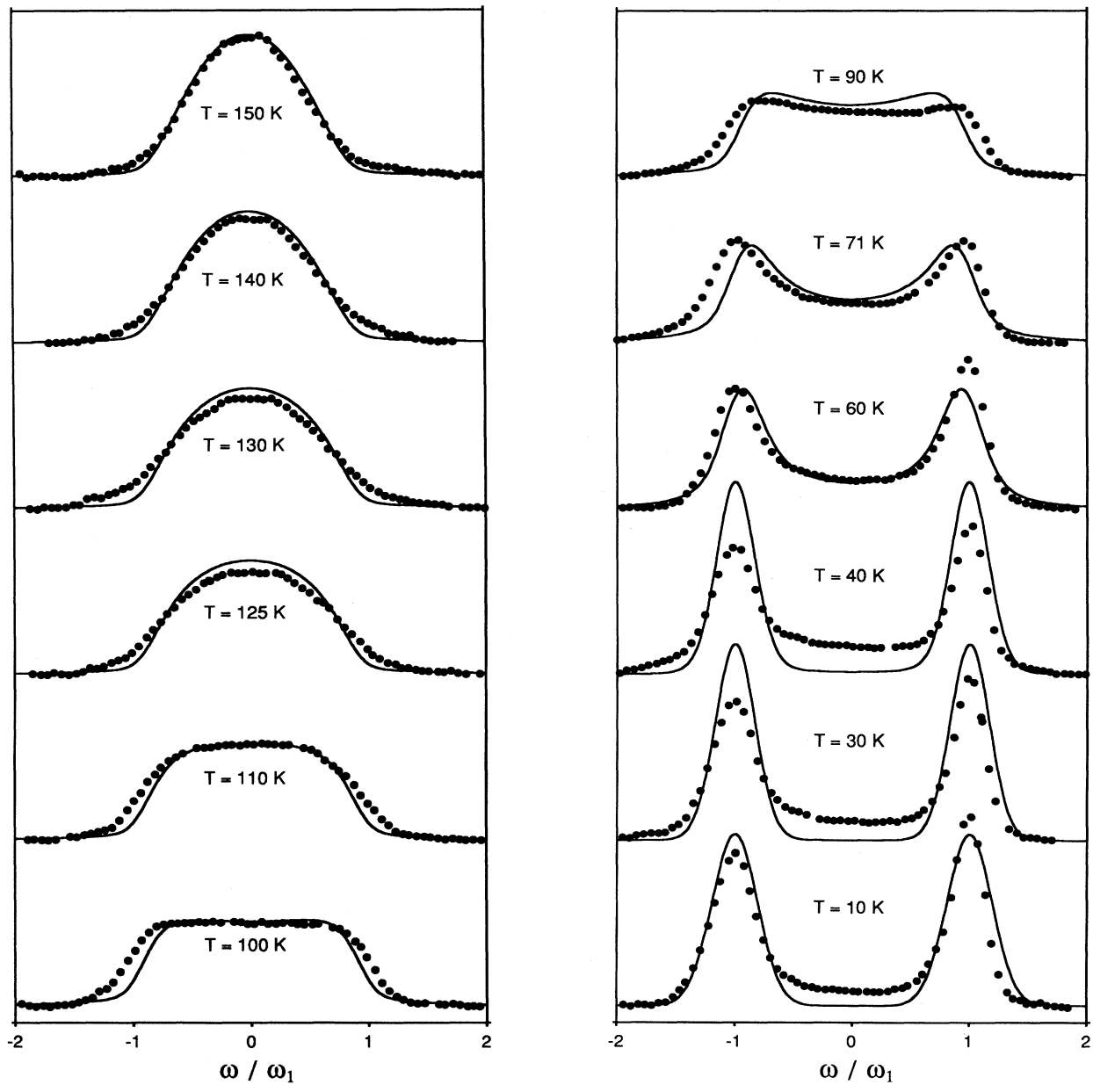

FIG. 4. Comparison between theoretical and experimental Tl^{2+} EPR line shapes at different temperatures, taking into account both static and dynamic effects. The calculations were performed using the fit parameters obtained from the second moment data.

ter q_{EA}. On the other hand, the nonlocal effects are here only a perturbation for which the central limit theorem can be applied, i.e., we can expect that these perturbations have a Gaussian probability distribution. An example of how this theorem works is shown in Ref. 5 where NMR line shapes resulting from the random distribution of Rb and NH_4 ions in RADP have been calculated. We now have to convolute our calculated line shape $I(\omega)$ with a Gaussian of variance (σ_0^2/q_{EA}). The value of σ_0 was obtained from the Tl^{2+} EPR line shape at 10 K. At this temperature $I(\omega)$ consists of two narrow peaks centered at $p=\omega/\omega_1=\pm 1$. The observed width of these peaks thus equals $2\sigma_0\sqrt{q_{EA}}$. From this we obtain $\sigma_0=90$ MHz. All experimental line shapes between 10 and 150 K can be now reproduced by using only the above five parameters. Some examples are shown in Fig. 4. The agreement between theory and experiment is remarkably good in view of the fact that the measured line shapes had to be digitized from analog plots.

There are, however, some minor but significant deviations of the experimental line shapes from the theoretical ones at intermediate temperatures which are due to the oversimplified model we have used for the kinetic slowing down. This is connected with the broad distribution of proton autocorrelation times in RADP already reported in Ref. 10. Though we have used site-dependent (p-dependent) autocorrelation times, the corresponding autocorrelation functions all have an exponential decay and thus the presently used distribution function of τ_c is much too narrow despite the divergence at $p=1$. This divergence has only a marginal influence on the line shape because, for $p>0.99$ ($\tau_c<\tau_0/7$), there is almost no difference between the fast-motion limit (where the narrow peak is centered between $0.99\times\omega_1$ and ω_1) and the slow-motion limit (where the main peak is centered at ω_1 and the peak at $-\omega_1$ has an intensity of less than 0.5%). A much larger effect on the line shape has a distribution of correlation times for small values of the local polarization p [where the function $I(\omega,p)$ is broadest], i.e., a distribution of τ_0. On lowering the temperature from 150 K, the deviation from the single τ_0 calculation should first be observed in the wings of the line due to the leading slow-motion edge of the τ_0 distribution. This can indeed be observed, e.g., on the 130- and 125-K line shapes where we have more intensity in the wings. On the other hand, at low temperatures the passing of the fast-motion edge should be visible in the center of the spectrum. Typical for this behavior are the experimental line shapes at 40, 30, and 10 K, respectively. Here we have to restrict ourselves to the qualitative statement that we can observe the distribution of the correlation times τ_0 in the temperature dependence of the Tl^{2+} EPR line shapes of RADP. For a quantitative determination of this distribution, the EPR measurements are not suitable.

Finally, we wanted to know whether there is really no sign of dynamics in the two-clock experiment as indicated by a qualitative inspection of the line splittings shown in Fig. 1. In Fig. 5(a) we show the measured temperature dependence of the second moments M_{2L} and M_{2H} of the Tl^{2+} EPR low-field and high-field line shapes and in Fig. 5(b) the corresponding ratios M_{2H}/M_{2L}. Though there is not much of a scatter to be seen in the second moments, the scatter in their ratio is quite large, so that one can only say that this ratio is indeed decreasing with decreasing temperature. Knowing that $M_{2L}(T)$ and $M_{2H}(T)$ are smooth functions of temperature, we have applied a linear regression fit to both sets as shown in Fig. 5(a). The solid curve shown in Fig. 5(b) is obtained from the ratio of the two fits. This line now beautifully demonstrates the presence of the kinetic slowing down in the two-clock experiment which cannot be seen from the line splittings. The fitted $M_{2H}/M_{2L}=f(T)$ curve has the correct sign of the slope and the correct curvature $-f(T)$ should converge to a horizontal line at $(\omega_{1H}/\omega_{1L})^2$ in the slow-motion limit, in agreement with the predictions made in Sec. III.

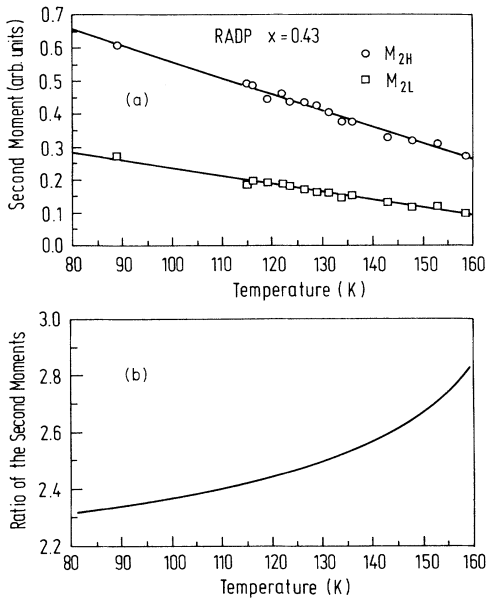

FIG. 5. (a) Temperature dependence of the second moments M_{2L} and M_{2L} of the Tl^{2+} low- and high-field EPR line shapes. (b) Temperature dependence of the ratio of the corresponding second moments M_{2L}/M_{2L}.

V. CONCLUSIONS

A comparison of experimental and theoretical singlet and doublet Tl^{2+} EPR line shapes and second moments between 160 and 10 K has shown the following.

(i) The transition from the fast- to the slow-motion regimes occurs here at a much higher temperature than observed previously[1] by NMR. This is the result of the fact that the Tl^{2+} EPR doublet splittings are much larger than the corresponding doublet splittings in ^{87}Rb and deuteron NMR. The EPR line shape is therefore sensitive to dynamic effects over the whole investigated temperature range, whereas, in NMR, dynamic effects are important only at low temperatures.

(ii) No agreement between experimental and theoretical

line shapes can be obtained if only static or only dynamic aspects of the glass transition are taken into account. A rather good agreement has been, however, obtained when both dynamic and static features of the glass transition are taken into account using the recently developed[2] dynamic approach to the local polarization distribution and magnetic resonance line shapes in proton glasses.

(iii) The static features of the glass transition can be described by a random-field smearing at a random-bond Ising pseudo-spin-glass transition with $T_G=30$ K and $T_f=60$ K, whereas the dynamic features show up in a slowing down of the proton intra- O—H $\cdots$ O bond motion. This slowing down of the proton motion can be, in a first approximation, described by an activation energy of $E_a=24$ meV and an inverse attempt frequency of $\tau_\infty=7.6\times10^{-12}$ s.

(iv) The above model for proton motion is certainly oversimplified as shown by some minor, but significant, deviations between experimental and theoretical line shapes at intermediate temperatures. The deviations can be qualitatively explained by assuming a broad distribution of proton autocorrelation times but a quantitative determination of these distributions from EPR measurements is not possible.

Finally, one should stress that the comparison of the results of this work with that of Ref. 1 shows an interesting isotope effect in the nominal glass-transition temperatures of deuterated and undeuterated RADP. For RADP we find $T_G=30$ K and $T_f=60$ K, whereas we have, for DRADP, $T_G=90$ K and $T_f=53$ K. This means that deuteration does not affect the variance of the random-field distribution $\Delta=(k_B T_f)^2$, whereas it affects the nominal pseudo-spin-glass temperature T_G. The isotope effect $T_{G,D}/T_{G,H}=3$ is here significantly larger than the one in KH_2PO_4 where $T_{C,D}/T_{C,H}=1.57$.

ACKNOWLEDGMENTS

This work was supported in part by the Swiss National Science Foundation and by the Research Council of Slovenia (Yugoslavia).

*On leave from Jožef Stefan Institute, Ljubljana, Yugoslavia.

[1]R. Blinc, J. Dolinsek, R. Pirc, B. Tadic, B. Zalar, R. Kind, and O. Liechti, Phys. Rev. Lett. **63**, 2248 (1989).

[2]R. Pirc, B. Tadic, R. Blinc, and R. Kind, Phys. Rev. B **43**, 2501 (1991).

[3]R. Pirc, B. Tadic, and R. Blinc, Phys. Rev. B **36**, 8607 (1987).

[4]E. Courtens, Jpn. J. Appl. Phys. **24**, 70 (1985), and references therein.

[5]R. Kind, R. Blinc, and M. Koren, Phys. Rev. B **37**, 4864 (1988).

[6]R. Kind, O. Liechti, and M. Mohr, Ferroelectrics **78**, 87 (1988).

[7]P. Cevc, B. Zalar, and R. Blinc, Solid State Commun. **70**, 461 (1989).

[8]K. Binder and A. P. Young, Rev. Mod. Phys. **58**, 801 (1986).

[9]K. B. Binder, Ferroelectrics **104**, 3 (1990).

[10]J. Slak, R. Kind, R. Blinc, E. Courtens, and S. Zumer, Phys. Rev. B **30**, 85 (1984).

[11]R. Blinc, B. Günther, and D. C. Ailion, Phys. Scr. **T13**, 205 (1986).

[12]R. Blinc, D. C. Ailion, B. Günther, and S. Zumer, Phys. Rev. Lett. **57**, 2826 (1986).

[13]L. V. Gonzaga, J. F. Sampaio, G. M. Ribeiro, A. S. Chaves, R. Gazzinelli, and R. Blinc, J. Phys. Soc. Jpn. **51**, 540 (1982).

[14]V. N. Efimov, N. I. Silkin, V. G. Stepanov, and L. A. Trofanchuk, Fiz. Tverd. Tela **21**, 2355 (1979) [Sov. Phys.—Solid State **21**, 1464 (1979)].

[15]R. Blinc, P. Cevc, and S. Zumer, Solid State Commun. **66**, 319 (1988).

[16]R. Blinc, P. Cevc, and N. I. Silkin, Phys. Status Solidi B **127**, K147 (1989).

[17]P. Cevc (unpublished).

[18]R. Kind, M. Mohr, H. Looser, and O. Liechti, in *Proceedings of the 23rd Congress Ampere on Magnetic Resonance, Roma, 1986,* edited by B. Maraviglia, F. de Luca, and M. Campanella (Instituto Superiore di Sanita, Roma, 1986), p. 140.